IOP PUBLISHING
IOP FTC
JOURNAL OF PHYSICS D: APPLIED PHYSICS
J. Phys. D: Appl. Phys. **41** (2008) 032005 (4pp)
doi:10.1088/0022-3727/41/3/032005

FAST TRACK COMMUNICATION

Spatial coupling of particle and fluid models for streamers: where nonlocality matters

Chao Li[1], **Ute Ebert**[1,2], **W J M Brok**[1,2] **and Willem Hundsdorfer**[1]

[1] CWI, PO Box 94079, 1090 GB Amsterdam, The Netherlands
[2] Department of Applied Physics, Eindhoven University of Technology, PO Box 513, 5600 MB Eindhoven, The Netherlands

Received 16 October 2007, in final form 12 December 2007
Published 8 January 2008
Online at stacks.iop.org/JPhysD/41/032005

Abstract
Particle models for streamer ionization fronts contain correct electron energy distributions, runaway effects and single electron statistics. Conventional fluid models are computationally much more efficient for large particle numbers, but create too low ionization densities in high fields. To combine their respective advantages, we here show how to couple both models in space. We confirm that the discrepancies between particle and fluid fronts arise from the steep electron density gradients in the leading edge of the fronts. We find the optimal position for the interface between models that minimizes the computational effort and reproduces the results of a pure particle model.

(Some figures in this article are in colour only in the electronic version)

Streamers generically occur in the initial electric breakdown of long gaps. They are growing filaments of weakly ionized nonstationary plasma; they are produced by a sharp ionization front that propagates into nonionized matter within a self-enhanced electric field. Streamers are used in industrial applications such as lighting [1], gas and water purification [2, 3] or combustion control [4], and they occur in natural processes as well, such as lightning [5,6] or transient luminous events in the upper atmosphere [7, 8]. Recent important questions concern (i) propagation and branching of streamers [9] and the role of avalanches created by single electrons, (ii) the electron energy distribution in the streamer head and the subsequent gas chemistry that is used in the above applications as well as (iii) runaway electrons and x-ray generation, possibly in the streamer zone of lightning leaders [10, 8]. This paper deals with efficient simulation of these problems.

Monte Carlo particle simulations [11, 12] model these effects as they contain the full microscopic physics; the deterministic electron motion between collisions is calculated and collisions of electrons with neutrals are treated through a Monte Carlo process with appropriate statistical weights. The particle model includes the complete electron velocity and energy distribution as well as the discrete nature of particles. However, a drawback of such models is that the required computation resources grow with the number of particles and eventually exceed the CPU space of any computer. This difficulty is counteracted by using superparticles carrying the charge and the mass of many physical particles, but superparticles in turn create unphysical fluctuations and stochastic heating [13].

Streamers are therefore mostly modelled as fluids (see, e.g. [14–18]) since a fluid model is computationally much more efficient. In the case of a negative discharge in a pure nonattaching gas such as nitrogen, it consists of continuity equations for the densities of electrons n_e and positive ions n_p coupled to the Poisson equation for the electric field $\boldsymbol{E}$. The electron mobility μ and diffusion matrix $\boldsymbol{D}$ and the impact ionization rate α are calculated from microscopic scattering and transport models such as the Boltzmann equation [19] or directly from Monte Carlo simulations as, e.g. in [20]. In streamer calculations, it is generally assumed that these transport and reaction coefficients are functions of the local electric field.

We have recently compared the properties of streamer ionization fronts of particle models and conventional fluid models [20] for negative planar fronts in nitrogen; the transport coefficients for the fluid model were generated from swarm experiments in the particle model. We found that the models agree reasonably for fields up to $50\,\mathrm{kV\,cm^{-1}}$ at standard temperature and pressure, but that differences increase with increasing electric field. For example, in a field of $200\,\mathrm{kV\,cm^{-1}}$, the ionization level behind the front is 60% higher in the particle model than in the fluid model. We have related this to the fact that the electron energies and, consequently, the ionization rates in the leading edge of the front are considerably higher in the particle than in the fluid model; they are actually at the edge of the runaway. We found that this effect is due to the strong density gradients in the front, and not due to field gradients. So for high fields and consequently strong density gradients at the streamer tip, there is a clear need for particle simulations, and particles, rather than superparticles, should be used to get physically realistic density fluctuations when modelling, for example, the branching process of a streamer.

The basic idea of this paper is demonstrated in figure 1, namely, to follow the single electron dynamics in the high field region of the streamer where the electron density gradient is steep and to present the interior region with large numbers of slower electrons through a fluid model with appropriate transport coefficients. As in [20], we study negative streamers in nitrogen, and we simplify the notation by referring to the standard temperature and pressure though the model trivially scales with the gas density. The particle and the fluid models by themselves are taken as described in detail in [20]. But how should the particle and fluid models be coupled in space? And where should the interface between the models be located to get fast but reliable results? The answers to these questions will be given below. They required us to correctly identify the spatial region where the particle and fluid models deviate, and this allowed us to then compute the full electron physics efficiently in the relevant region.

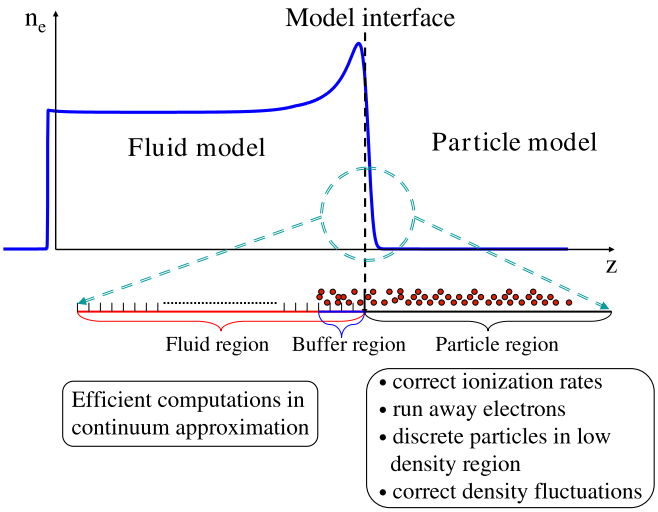

Figure 1. The streamer ionization front, that is here indicated by the electron density $n_e(z)$, and its presentation by the particle or the fluid model in different spatial regions.

When coupling the models, the model interface should move with the ionization front; this keeps the total number of electrons limited and superparticles need not be introduced. The position of the interface can be chosen according to either the electron densities or the electric field. As the electron densities fluctuate stronger than the electric field, we relate the position of the model interface to the electric field. More precisely, the interface is placed where the local field E is a given fraction x of the maximal field E^+: $E_{\mathrm{interface}} = x\,E^+$. By varying x, the region modelled by particles can be varied.

To properly handle the interaction of the two models, we introduced a so-called 'buffer region' where a particle model coexists with a fluid model. The separation of the full computational region into fluid, particle and buffer regions is indicated in figure 1. Buffer regions have been introduced in [21–23] for rarefied gases coupling a direct simulation Monte Carlo (DSMC) scheme to the Navier–Stokes equations and in other applications [24, 25]. Physical observables are evaluated from the fluid model in its whole definition region up to the model interface. Beyond that point, the particle model is used. The particle model extends back beyond the model interface into the buffer region where particle and fluid models coexist; it supplies particle fluxes to the fluid model on the model interface. However, correct particle fluxes require correct particle statistics within the buffer region whose length should be as small as possible to reduce computation costs, but larger than the electron energy relaxation length [20]. In many cases, new particles need to be introduced into the buffer region, which have to be drawn from appropriate distributions in the configuration space. This would pose a particular problem since a Boltzmann or even a Druyvesteyn distribution can be inaccurate. But for negative streamers, where electrons on average move somewhat slower than the ionization front, the electron loss at the end of a sufficiently long buffer region does not affect the calculation of particle fluxes at the model interface. Therefore, the particle loss at the end of the buffer region can be ignored and new electrons do not need be created artificially.

In more detail, the calculation is performed as follows. One hybrid computation step from t_n to t_{n+1} is described in the flow chart in figure 2. The electric field E, the electron

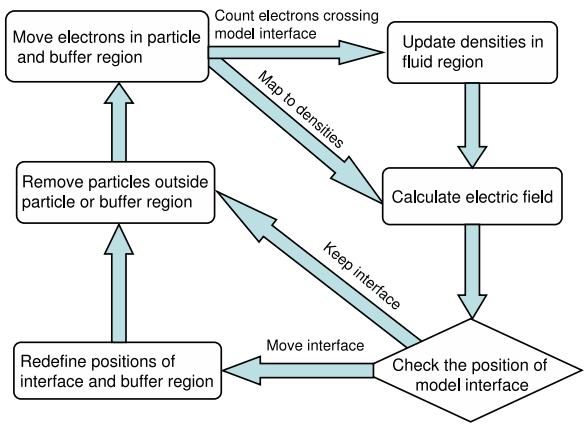

Figure 2. Flow chart for one time step from t_n to t_{n+1} in the complete hybrid calculation.

and ion densities n_e and n_p in the fluid region and the kinetic information of particles in the particle and buffer regions are given at time step t_n. First, the positions and velocities of all old and newly generated particles are updated to time step t_{n+1} in the particle and buffer regions. Their collisions during this time step are treated stochastically and their new velocities and positions are calculated by solving the equation of motion. The number of electrons crossing the model interface during this time step is recorded. This particle flux across the interface provides the required boundary condition for calculating the evolution of the densities in the fluid region up to the same time t_{n+1}. The particles are at arbitrary positions, but densities and field are calculated here on the same numerical grid. Therefore, the particles in the particle region are averaged to densities on the numerical grid, and then the electric field at time t_{n+1} is calculated from the Poisson equation everywhere. (The charge density in the buffer region is taken from the fluid model, and the particles in the buffer region only serve to generate correct fluxes for the fluid region.) Finally, the position of the model interface is updated to its new position at time t_{n+1}; it can stay where it was or move one grid size forward. The buffer region moves with it. All particles that are now neither in the particle nor in the buffer region are removed from the particle list.

In the particle model, a standard particle in cell/Monte Carlo collision (PIC/MCC) method is implemented. At each time step of length $\Delta t = 0.3$ ps, particles in the particle regions are mapped to densities on a uniform grid with a mesh size of $\Delta\ell = 2.3\,\mu$m. Meanwhile, the fluid equations are solved in the fluid region of the same grid; discretization and grid dependence of the fluid model are discussed in detail in [14]. The charge density $n_p - n_e$ then can be obtained everywhere and the electric field is calculated on this grid. The size of the time step and the grid size are chosen such that the ionization front need several time steps to move over one $\Delta\ell$, e.g. $10\Delta t$ at 100 kV cm^{-1} and $3\Delta t$ at 200 kV cm^{-1}.

The length of the buffer region is another crucial factor in the hybrid computation. A buffer region with a length of $32\Delta\ell$ has been used in the current simulations, which ensure a reliable flux around the model interface and stable results of hybrid simulations. The length of the buffer region is much larger than the energy relaxation length found in [20]. The long buffer region does not bring a heavy burden to the simulation of the planar front system but will considerably reduce the computational efficiency in a more complex geometry. Therefore, the minimal length of the buffer region as well as other features of fluid and particle models shall be investigated in more detail in a future paper.

We first show the simulation results of this coupled model for a front propagating into a field of $E^+ = -100$ kV cm^{-1}, and with the model interface located at $x = 0.6$, 0.9 and 0.98; the positions of these interfaces are indicated in figure 3. The field ahead of the front is fixed, and the system is always taken long enough such that effects at the outer boundaries are not felt. The coupled model generates different electron and ion densities behind the ionization front as shown in figure 4; for $x = 0.6$, the density is as in the particle model, for $x = 0.98$, it is as in the fluid model, and for $x = 0.9$, it takes some intermediate value. We conclude that the solution of the pure

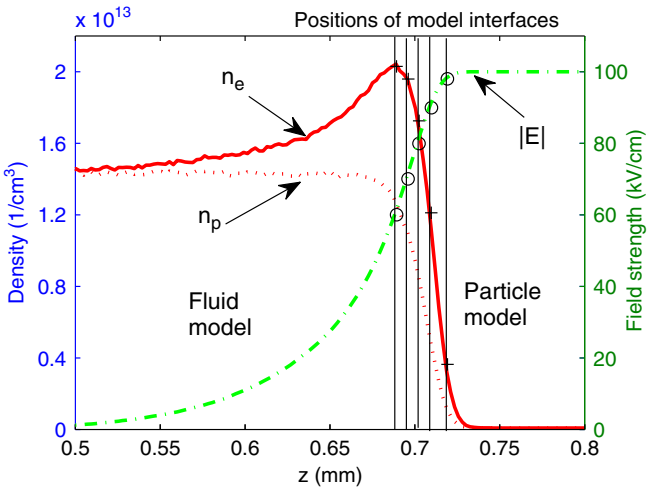

Figure 3. Electron density n_e and ion density n_p (solid and dotted lines) and electric field strength $|E|$ (dashed–dotted line) in a streamer ionization front in nitrogen in a field of $E^+ = -100$ kV cm^{-1} at standard temperature and pressure within a pure particle model. Our units are related to other commonly used units such as 1 kV cm^{-1} bar^{-1} = 1.316 V cm^{-1} Torr^{-1} = 0.424 Td at $T = 300$ K. Below we will model the leading edge of the front by a particle model and the streamer interior by a fluid model where the model interfaces are located at $E_{\text{interface}} = x\,E^+$ with $x = 0.6$, 0.7, 0.8, 0.9 and 0.98. These interface positions for figures 2 and 3 are marked by vertical lines, with 'o' for the fields and with '+' for the densities.

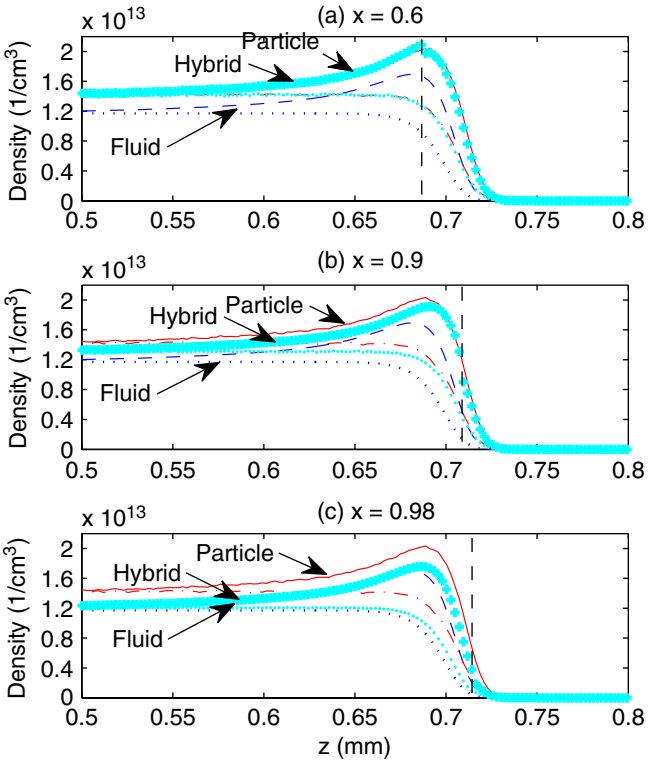

Figure 4. Electron and ion densities in the coupled model (thick lines) in a field of $E^+ = -100$ kV cm^{-1} with model interfaces at $E_{\text{interface}} = x\,E^+$ with (*a*) $x = 0.6$, (*b*) $x = 0.9$ and (*c*) $x = 0.98$; these interface positions are indicated by vertical dashed lines. The densities in the particle model (electrons: solid, ions: dotted–dashed) and in the fluid model (electrons: dashed, ions: dotted) are shown as well; they are discussed in [20].

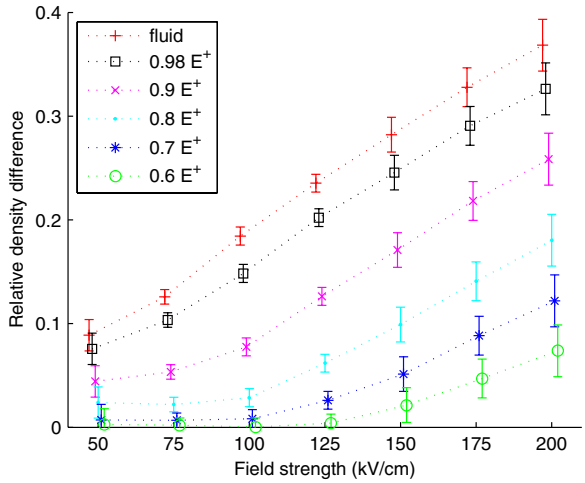

Figure 5. Relative density difference behind the front $(n^-_{\mathrm{e,part}} - n^-_{\mathrm{e,coup}})/n^-_{\mathrm{e,part}}$ between the particle model and the coupled model as a function of the applied electric field E^+ and of the position of the model interface $E_{\mathrm{interface}} = x \cdot E^+$ with $x = 0.6$ (□), 0.7 (x), 0.8 (·), 0.9 (∗), 0.98 (○) and 1.0 (+). The last case corresponds to the fluid model. (Note that a density difference of 60% relative to the fluid model corresponds to a density difference of 37.5% relative to the particle model.)

particle model can be replaced by the coupled model, if a sufficiently large region of the ionization front with its steep gradients is covered by the particle model, and that the coupling to the fluid model behind that region does not cause numerical artefacts. This confirms the discussion in [20]; it is indeed the high electron density gradient that causes an electron energy overshoot and a higher ionization rate in the leading edge of the particle front. The coupled model also confirms that the field gradients do not play a role in causing density discrepancy between the fluid and the particle model as the field keeps varying across the model interface in the coupled model.

Having analysed the ionization front propagating into a field of $E^+ = -100\,\mathrm{kV\,cm^{-1}}$, we now summarize the results for fields ranging from -50 to $-200\,\mathrm{kV\,cm^{-1}}$. Figure 5 shows the discrepancy between the particle and coupled models on the most sensitive observable [20], namely, on the relative difference $(n^-_{\mathrm{e,part}} - n^-_{\mathrm{e,coup}})/n^-_{\mathrm{e,part}}$ in the saturated electron density n^-_{e} behind the ionization front. This quantity is shown as a function of the electric field E^+ and of the position of the model interface parameterized again by x. The figure shows that for higher E^+, the parameter x needs to be smaller. This shift of the required interface position relative to E^+ corresponds to a shift of the maximal electron density relative to E: both for $E^+ = -50\,\mathrm{kV\,cm^{-1}}$ and for $E^+ = -200\,\mathrm{kV\,cm^{-1}}$, the particle and the coupled models agree well, if the model interface lies at the maximum of the electron density and therefore covers the complete steep gradient region; this is the case at $E = 0.8E^+$ for $E^+ = -50\,\mathrm{kV\,cm^{-1}}$ and at $E = 0.35E^+$ for $E^+ = -200\,\mathrm{kV\,cm^{-1}}$.

Coupling particle and fluid models in space with varying interface positions confirms our prediction [20] that the density discrepancies between particle and fluid model are due to strong density gradients in the leading edge of the front. This investigation also lays the basis for constructing a fully 3D coupled particle–fluid model where the fields ahead of the ionization front are changing in space and time.

Acknowledgment

The authors acknowledge the support of the Dutch National Programme BSIK, in the ICT project BRICKS, theme MSV1.

References

[1] Bhoj A and Kushner M J 2005 *IEEE Trans. Plasma Sci.* **33** 518
[2] Winands G J J, Liu Z, Pemen A J M, van Heesch E J M, Yan K and van Veldhuizen E M 2006 *J. Phys. D: Appl. Phys.* **39** 3010
[3] Grabowskin L R, van Veldhuizen E M, Pemen A J M, and Rutgers W R 2007 *Plasma Sources Sci. Technol.* **16** 226
[4] Starikovskaia S M 2006 *J. Phys. D: Appl. Phys.* **39** R265
[5] Rakov V A and Uman M A 2003 *Lightning: Physics and Effects* (Cambridge: Cambridge University Press)
[6] Williams E R 2006 *Plasma Sources Sci. Technol.* **15** 91
[7] Sentman D D, Wescott E M, Osborne D L, Hampton D L and Heavner M J 1995 *Geophys. Res. Lett.* **22** 1205
[8] Pasko V P 2007 *Plasma Sources Sci. Technol.* **16** 13
[9] Ebert U, Montijn C, Briels T M P, Hundsdorfer W, Meulenbroek B, Rocco A and van Veldhuizen E M 2006 *Plasma Sources Sci. Technol.* **15** S118
[10] Dwyer J R *et al* 2003 *Science* **299** 694
[11] Brok W J M, Wagenaars E, van Dijk J and van der Mullen J J A M 2007 *IEEE Trans. Plasma Sci.* **35** 1325
[12] Chanrion O and Neubert T 2007 *J. Comput. Phys.* submitted
[13] Li C, Ebert U and Brok W J M 2007 *IEEE Trans. Plasma Sci.* submitted, *Preprint* arXiv:0712.1942
[14] Montijn C, Hundsdorfer W and Ebert U 2006 *J. Comput. Phys.* **219** 801
[15] Ségur P, Bourdon A, Marode E, Bessieres D and Paillol J H 2006 *Plasma Sources Sci. Technol.* **15** 648
[16] Moss G D, Pasko V P, Liu N and Veronis G 2006 *J. Geophys. Res.* **111** A02307
[17] Liu N and Pasko V P 2006 *J. Phys. D: Appl. Phys.* **39** 327
[18] Luque A, Ebert U, Montijn C and Hundsdorfer W 2007 *Appl. Phys. Lett.* **90** 081501
[19] Hagelaar G J M and Pitchford L C 2005 *Plasma Sources Sci. Technol.* **14** 722
[20] Li C, Brok W J M, Ebert U and van der Mullen J J A M 2007 *J. Appl. Phys.* **101** 123305
[21] Garcia A L, Bell J B, Crutchfield W Y and Alder B J 1999 *J. Comput. Phys.* **154** 134
[22] Alexander F J, Garcia A L and Tartakovsky D M 2002 *J. Comput. Phys.* **182** 47
[23] Alexander F J, Garcia A L and Tartakovsky D M 2005 *J. Comput. Phys.* **207** 769
[24] Delgado-Buscalioni R and Coveney P V 2003 *Phys. Rev.* E **67** 046704
[25] Aktas O and Aluru N R 2002 *J. Comput. Phys.* **178** 342